Dissociative decay of $n=3$ levels in H_2. II. Excited by laser from the metastable $c\,^3\Pi_u^-$ state of H_2

D. P. de Bruijn* and H. Helm†
Stichting voor Fundamenteel Onderzoek der Materie Institute for Atomic and Molecular Physics, Kruislaan 407, 1098 SJ Amsterdam, The Netherlands
(Received 7 April 1986)

Fast-beam photofragment spectroscopy has been applied to study the photodissociation of metastable H_2 molecules in the $c\,^3\Pi_u^-$ state, formed by charge exchange of H_2^+ with Cs vapor. Transitions leading to radiatively dissociated or predissociated levels of the *g*, *h*, *i*, and *j* triplet *gerade* states of H_2 are observed. The decay mechanisms, level positions, and, in the case of predissociations, the lifetimes are established for (ro-)vibrational levels ($v \geq 4$). The transitions to $v \geq 5$ levels of the $j\,^3\Delta_g$ state appear as asymmetric peaks with widths of around 50 cm^{-1} ($N=2$). A calculation of the rotational coupling of the *j* state to the vibrational continuum of the $i\,^3\Pi_g$ state confirms this very rapid predissociation ($\tau \simeq 10^{-13}$ s). For $v=4$ of the *j* state, which couples to the continuum via the quasibound $v=5$ level of the *i* state, a relatively slow predissociation ($\tau \simeq 10^{-8}$ s) is observed.

I. INTRODUCTION

Recently we have reported[1] about a novel technique: fast neutral-beam photofragment spectroscopy, applied to the metastable $c\,^3\Pi_u^-$ state of H_2. This paper is intended to give a full account of these measurements, which cover the excitation range from 565–635 nm. In this range the $n=3$ levels of H_2 are accessed. The preceding paper (paper I)[2] also deals with dissociative $n=3$ levels in H_2 but populated in charge-exchange collisions. For a short review on the spectroscopy of these states we refer to the introduction of that paper. By using charge exchange to create a fast neutral beam, photodissociation in neutral molecules can be studied with the high resolution of translational spectroscopy. This is particularly advantageous if one is able to populate a metastable molecular state with a symmetry which is different from the ground state. Here the $c\,^3\Pi_u^-$ state is used, from where triplet states can be excited which cannot be reached from the singlet ground state by optical means. For this kind of photodissociation spectroscopy one needs a special experimental version of translational spectroscopy, such as the two-particle detector which we developed a few years ago,[3] because both fragments are neutral. With this technique we have already performed detailed experiments on dissociations occurring during or directly after charge-exchange collisions of H_2^+ (Ref. 4), among them the predissociation of the $c\,^3\Pi_u^+$ state of H_2 (Refs. 5 and 6). From these experiments the population of the predissociative Π^+ state, the upper Λ-doublet component, is deduced. If we assume that the charge-exchange process is not selective in the Λ-doublet component, the population of the metastable Π^- levels may be inferred from these measurements. The lifetimes of the Π^- levels are 1 ms for $v=0$ and 0.1 ms for $v \geq 1$ (Refs. 7 and 8). With a Cs charge-exchange target and H_2^+ extracted from an electron-impact ion source, we obtain an H_2 beam mainly in the $c\,^3\Pi_u^-$ state. All vibrational levels are populated and the rotational temperatures are rather low (300 K for $v=0$).

The unique possibility to study triplet gerade Rydberg states in H_2 by single-photon absorption from the metastable *c* state has recently already been utilized by Eyler and Pipkin.[9] By electron-impact excitation of H_2 they

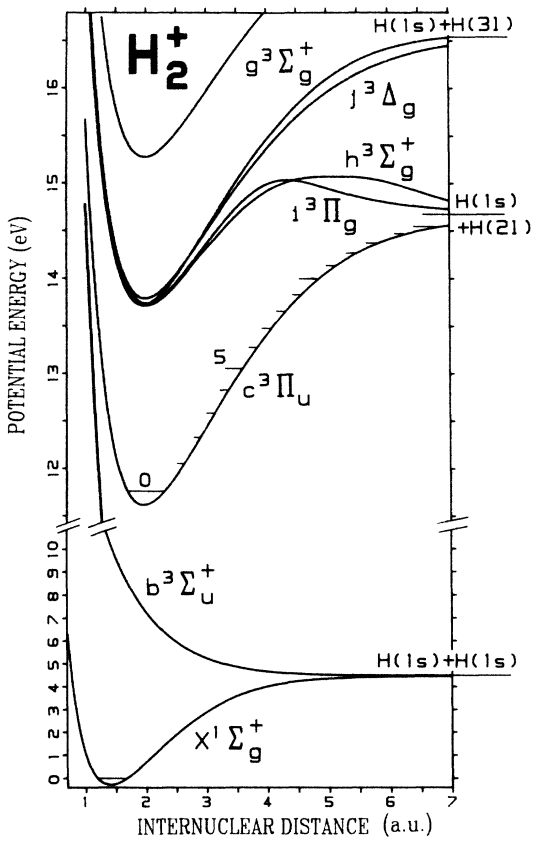

FIG. 1. Relevant potential curves of H_2, taken from Sharp (Ref. 16) and Kolos and Rychlewski (Refs. 17 and 21). All existing triplet gerade $n=3$ Rydberg states, which can be excited with one visible photon from the metastable $c\,^3\Pi_u$ state, are shown.

populated the c state and measured the fluorescence after subsequent laser excitation. In this way the lifetimes of the lowest vibrational ($v=0,1$) and rotational levels for all four $n=3$ triplet gerade states in para-H_2 (the $g\,^3\Sigma_g^+$, $h\,^3\Sigma_g^+$, $i\,^3\Pi_g$, and $j\,^3\Delta_g$ states) could be measured,[9] most of them yielding values between 10 and 20 ns. These levels, all below the H(1s)+H(2l) dissociation limit, decay to the repulsive $b\,^3\Sigma_u^+$ state (see Fig. 1). The 3s and 3d complex of H_2, formed in the triplet case by, respectively, the h and the g, i, j states, has further been the subject of extensive theoretical studies because it exhibits extreme Λ-type doubling.[10] Other observations of these states, also only for the lower v's were performed in gas discharges. In the extensive work of Dieke[11,12] emission lines to the $c\,^3\Pi_u$ state are given, while Herzberg[13] has reported absorption transitions originating in the $c\,^3\Pi_u^-$ levels.

In this work transitions from the c state to the g, h, i, and j triplet gerade states, including levels above the H(1s)+H(2l) dissociation limit, are observed. All these levels, besides radiating back to the c state, primarily lead to dissociation, either after radiative decay to the b state or through various types of predissociation. Detecting dissociations is therefore an obvious way to study these states. Also levels with very short predissociative lifetimes, as we have observed for $v=5$–9 of the j state, can be detected in this way.

II. EXPERIMENTAL PROCEDURE

The principle of the experimental method used here is the correlated detection of both fragments formed in a photodissociation event in a fast beam. A position- and time-sensitive double microchannel plate detector is used, which has been described in detail before.[3,5] A short explanation of the technique can be found in paper I.

A sketch of the new apparatus, which has a total length of 6 m, is given in Fig. 2. Except for the first vacuum chamber, which contains the ion source and part of the ion optics, all chambers can be moved on rails to facilitate changes in the setup. The vacuum system is divided into three parts, separated by adjustable beam diaphragms. The first part (ion source) has a working pressure of about 10^{-6} Torr, the second one of 5×10^{-8} Torr while the third one operates at 10^{-9} Torr. The low pressure in the last section is crucial to suppress background due to collision-induced dissociations.

A. Ion optics

The ion source used here is an electron-impact source (a in Fig. 3), used at a pressure of typically 1 mTorr of H_2 and operated at an electron energy of 100 eV. The ion optics consists of a three-element lens (einzellens, b), a Wien filter (d) for mass selection, an immersion lens (f) for post acceleration (up to 20 keV), and a second einzellens (h). The first einzellens extracts a beam up to 10 keV and focuses the velocity-selected ion beam upon the first diaphragm (e, 0.3–0.5 mm diam. in normal operation). This focus lies very close to the gap of the (post-accelerating) immersion lens. In this case the virtual image of the immersion lens is always located at (almost) the same position, independent of the accelerating voltage. This creates optimal conditions to refocus the beam with the second einzellens on the detector (o), where it is collected by a Faraday cup of 2 mm diameter. The flight length between the interaction center (l) and the detector can be varied from 25 cm to 2.5 m by choosing the length and number of vacuum chambers. The second diaphragm (k) regulates the accepted beam angle.

By the use of a Wien filter for mass (velocity) selection a straight beam line is obtained. Since all important elements (lenses and diaphragms) are movable with manipulators, alignment is relatively easy. The settings of the various deflection plates (c,g) is normally close to zero. In the last section the earth magnetic field is shielded by two concentric μ-metal cylinders (n) inside the vacuum chamber. The residual magnetic field is less than 1 mG, allowing accurate translational spectroscopy also on charged fragments. In the present experiments this option has not been exploited, only neutral H-H pairs are detected.

B. Photofragment spectroscopy

In the present configuration a collision chamber (Fig. 2, i) of 1 cm length, connected to an oven, is mounted after the second einzellens. Here about 5% of the H_2^+ beam (typically 10^{-10} A in the Faraday cup at the detector) is neutralized. Both Cs and Rb vapor have been utilized for charge transfer during the experiments, yielding identical results. A set of deflection plates (j) sweeps residual ions out of the beam and after a diaphragm (k) of 0.5 mm diameter a beam of neutral H_2 molecules is left. The flight length of 30 cm between the exchange cell and the laser crossing (about 0.35 μs flight time at 7.5 keV) allows radiative and dissociative decay of most of the excited H_2 states. Mainly the metastable levels of the $c\,^3\Pi_u$ state and the ground state will be populated.[2,4] This beam crosses perpendicularly with the intracavity photon beam of a dye laser (q) which is pumped by a 5-W Ar-ion laser (all lines). The intracavity photon flux is about 20 W at the top of the Rhodamine 6G dye tuning curve. The bandwidth of the dye laser, limited by a three-plate birefringent filter, is 40 GHz (about 1 cm^{-1}). The polarization of the laser was kept perpendicular to the neutral beam and thereby parallel to the open sectors[3,5] (the opening angles were 30°) of the two-particle detector. This introduces a preference for parallel transitions, i.e., a $\cos^2\theta$ distribution with respect to the laser polarization in a pure case.

The flight length to the detector is 154 cm in this experiment. The final positioning of the detector before an experiment is performed, is done by symmetrizing the spatial fragment patterns on both halves of the detector in combination with maximizing of the coincident count rate. An accuracy of 0.2 mm can be obtained in this way. About 15 cm after the crossing with the laser all fragments which enter the effective range of the detector, which has a central dead area of 10 mm diameter, have left the beam. At this position a (movable) V-shaped "beam flag" (m in Fig. 2) of 0.7 mm width was mounted which reduces the background from collision-induced and unimolecular dissociations by a factor of 10. Together

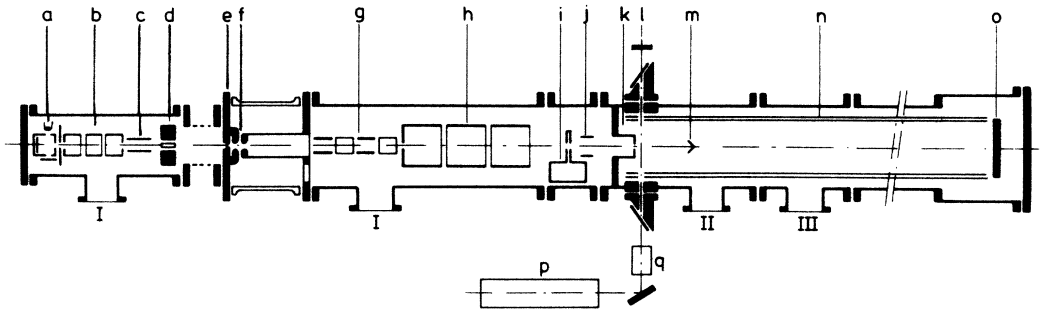

FIG. 2. Schematic drawing of the apparatus (see text).

with the 0.5 mm aperture (k) the beam flag selects a portion of the beam path which can be viewed by the detector. This simple device could therefore also be used to perform experiments on dissociative levels with very long lifetimes, such as shape resonances, where the dissociation does not occur at a fixed spot in the beam line.

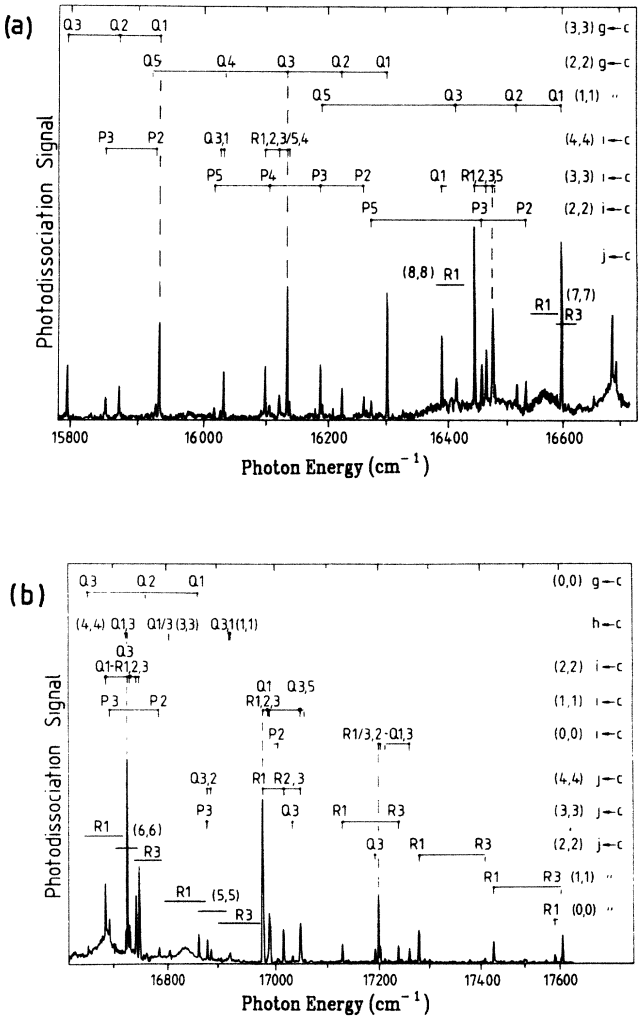

FIG. 3. Photodissociation signal as a function of the photon energy for a metastable H_2 beam. Background due to collision-induced dissociation has been subtracted.

III. EXPERIMENTAL RESULTS AND DISCUSSION

A. Wavelength spectrum

In Fig. 3 a spectrum of the photodissociation signal versus the photon energy is reproduced. The spectrum was recorded in about four hours by counting the number of coincidences on the detector while scanning the laser wavelength over the range of Rhodamine 6G dye with the birefringent filter. A background of dissociations due to collisional and unimolecular dissociation, amounting to about 1 kHz ($\simeq$20% of the highest peak in the spectrum), has been subtracted from the data. The partial laser output through a high reflector of the cavity was used for a first-order correction of the spectrum for the variation of laser power with wavelength. Because the exact transmission characteristics of this mirror are unknown, the relative peak heights may only be used in qualitative comparisons.

Over 50 discrete transitions appear in the photodissociation spectrum. Clear band structures are not apparent because of the large rotational and vibrational spacings in H_2. Many lines could be assigned directly on the basis of their photon energy, knowing the four possible upper states: the $g\,^3\Sigma_g^+$, $h\,^3\Sigma_g^+$, $i\,^3\Pi_g$, and $j\,^3\Delta_g$ states (presuming the $c\,^3\Pi_u$ state to be the only lower state). In Crosswhite's compilation[12] of Diekes emission spectra the levels of these states are given up to $v=3$ ($v=2$ for the h state). Only $\Delta v=0$ transitions appear because they are strongly favored by the Franck-Condon factors. The transitions which we have assigned and which have not been reported before are listed in Table I. The experimental photon energy scale was calibrated against known transitions given by Dieke, and is considered to be accurate to 1 cm^{-1}. The assignments will be elucidated in Secs. III C—III F separately for the four upper states.

B. Spectra of released kinetic energy

At 40 different photon energies, most of them on discrete transitions, spectra were taken of the released kinetic energy ε, in the center-of-mass frame. To obtain the highest resolution in ε we recorded only dissociations with a recoil angle θ close to 90°. This is achieved by assembling R spectra with the restriction $\tau<2$ ns and converting these (momentum) spectra into ε spectra.[5] With a beam energy of 7.5 keV, a flight length of 154 cm and 10

mm $< R <$ 40 mm (geometrical constriction of detector), the detectable range is 80 meV $< \varepsilon <$ 1.25 eV in this way. The absolute energy scale of the spectra was calibrated with known energy releases in the photodissociation of H_2 $c\,^3\Pi_u^-$ (see below) and is considered to be accurate within 10 meV. The energy resolution depends mainly on the resolution in R, amounting 100 μm, in accordance with Eq. (1). The best absolute resolution observed is 3 meV.

One can distinguish three different (photo)dissociation mechanisms: (i) *Direct dissociation* or "bound-free" transitions, (ii) *predissociations* or "bound-quasibound" transitions where finally the dissociative continuum is reached in a radiationless transition, and (iii) *radiative dissociations* if the initially excited discrete level radiates to a dissociative continuum, which can be denoted as "bound-bound-free" transitions. Only the first mechanism can be discriminated from the other two in a wavelength spectrum like Fig. 3. It produces a continuum instead of a discrete peak, which also means that it can easily be overlooked if the transition is weak. If ε spectra are added, however, all three mechanisms can very well be seen and discriminated from one another.

Predissociative lifetimes larger than a few nanoseconds can be measured from the exponential tail of the ε peak.[5] If the excited molecule lives for a significant time (relative to the flight time) before it dissociates, the flight length l to the detector becomes shorter and the apparent ε by that smaller. The effect is shown in Fig. 4 where the ε peak from a rather fast predissociation [$h \leftarrow c$ (4,4) $Q3$ transition, $\tau < 3$ ns] is plotted together with a peak due to a predissociation [$j \leftarrow c$ (4,4) $R1$ transition] with a lifetime of 9 ns and which almost coincides in ε. For very fast predissociations, lifetimes can be estimated from the width of the excitation transitions.

An example. In Fig. 5 a very instructive ε spectrum is shown, taken at a photon energy of 16 731 cm^{-1} where by coincidence all three dissociation mechanisms contribute within the bandwidth of the laser. The single sharp peak at 270 meV is due to a predissociation [mechanism (ii)], the measured value of ε corresponds to the energy of the

TABLE I. Observed new transitions from the metastable $c\,^3\Pi_u^-$ levels of H_2 to dissociative triplet gerade levels (see Figs. 1 and 3). Lines marked with an asterisk (*) are tentative assignments. The accuracy of the energies is about 1 cm^{-1}, equal to the bandwidth of the laser. The last two columns give, respectively, the observed and the calculated width Γ of the transition. If the observed width is not given it is smaller than 1 cm^{-1} (the bandwidth of the laser).

				Γ (cm^{-1})	
	(v',v)	Branch	$h\nu$ (cm^{-1})	Obs.	Calc.
$h \leftarrow c$	(3,3)	*$Q1$	16802		
		*$Q3$	16802		
	(4,4)	$Q1$	16729		
		$Q3$	16731		
$i \leftarrow c$	(3,3)	*$R5$	16479		
	(4,4)	$P2$	15926		1.4×10^{-3}
		$P3$	15851		2.5×10^{-3}
		$Q1$	16031		1.4×10^{-3}
		*$Q3$	16027		5.6×10^{-3}
		$R1$	16098		2.5×10^{-3}
		$R2$	16120		5.6×10^{-3}
		$R3$	16132		1.5×10^{-2}
		$R4$	16132		4.7×10^{-2}
		$R5$	16132		1.6×10^{-2}
$j \leftarrow c$	(4,4)	$Q2$	16878		0.2
		$Q3$	16871		0.8
		$R1$	16975		0.2
		$R2$	17015		0.8
		$R3$	17047		3
	(5,5)	$P3$	16600	>20	68
		$Q3$	16730	>20	130
		$R1$	16835	50 ± 10	68
		$R2$	16890	>20	130
		$R3$	16940	>20	204
	(6,6)	$Q2$	16600	>20	54
		$R1$	16680	50 ± 10	54
		$R2$	16720	>20	105
		$R3$	16750	>20	171
	(7,7)	$R1$	16565	50 ± 10	49
		$R3$	16600	>20	157
	(8,8)	$R1$	16400	>20	45
	(9,9)	$R1$	16300	>20	41

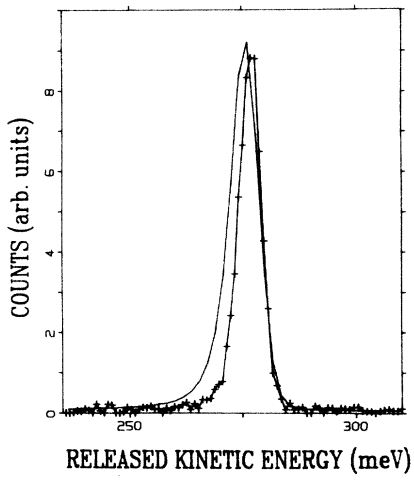

FIG. 4. Effect of predissociative lifetime τ on rotational peaks in the released kinetic energy. The narrowest peak at 269.5 meV (marked with a + for every mesh point) is the predissociation of the $v=4,N=3$ level ($Q3$ transition) of the $h\,^3\Sigma_g$ state with $\tau<3$ ns. The broader peak is due to the predissociation of the $v=4,N=2$ level ($R1$ transition) of the $j\,^3\Delta_g$ state, which has a lifetime of 9 ns. The latter peak has been shifted by 0.3 meV to coincide with the first peak and the continuous background has been subtracted from each peak.

excited discrete level above the dissociation limit. Together with the known photon energy the binding energy of the lower level in the transition can be calculated. In this case it is found that the lower level is $v=4,N=3$ of the $c\,^3\Pi_u^-$ state. Structures like the smaller peaks grouped together around 500 and 700 meV are in general (see comments in Sec. III F) caused by direct photodissociation [mechanism (i)]. In most cases the Franck-Condon factors for such a bound-free transition allow the photodissociation, at one wavelength, of several vibrational and a

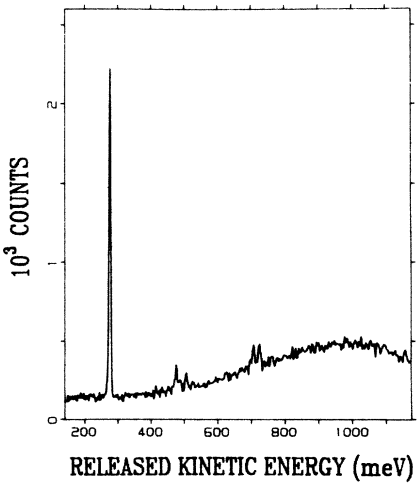

FIG. 5. Demonstration of the appearance of three different dissociation mechanisms in the spectrum of released kinetic energies. This is a spectrum of the photodissociation of metastable H_2 at 16731 cm^{-1}.

whole range of rotational levels. In this case the lower levels are several rotational levels (mainly the strongly populated $N=1$ and $N=3$ levels) of $v=5$ and $v=6$ of the c state. A radiative dissociation [mechanism (iii)] produces a continuum in ε because the repulsive final state can be reached over a whole range of internuclear distances. The continuum in Fig. 5, with a maximum around 1 eV, reflects a part of the vibrational wave function (the outer turning point) of the upper state.

C. The $g\,^3\Sigma_g^+$ ($3d\sigma$) state

We have observed the Q branches ($\Delta N=0$) of the $g\leftarrow c$ (0,0)-(3,3) bands. The selection rules (conservation of the para or ortho character) forbid P and R branches in this case (Ref. 13), $\Sigma_g^+\leftarrow\Pi_u^-$. The $Q1$ and $Q3$ transitions are strongest because they belong to strongly populated ortho levels. All observed levels ($v=0$–3) of the g state lie below the dissociation limit H(1s)+H(2l) and we have observed their decay by fluorescence to the repulsive $b\,^3\Sigma_u^+$ state (yielding a continuous ε spectrum). The exact level positions are given by Dieke,[11] provided the correction of -149.6 cm^{-1} for triplet states as found by Miller and Freund[14] is included. Transitions to higher vibrational levels of the g state lie outside the present wavelength range.

D. The $h\,^3\Sigma_g^+$ ($3s\sigma$) state

It is well known (see, e.g., Ref. 15, p. 133) that a $3s\leftarrow 2p$ transition is an order of magnitude weaker than $3d\leftarrow 2p$. Indeed the transitions to the $h(3s\sigma)$ state are observed to be weak (Fig. 3). Only the (1,1), the (3,3), and the (4,4) bands were detected in our experiment. Just as for the g state only Q branches are allowed when the h state is accessed from the metastable levels of the c state. The h state potential-energy curve is predicted to have a barrier[16] (Fig. 1) and supports five vibrational levels of which the upper two ($v=3$ and 4) lie above the dissociation limit and are therefore only quasibound. Only the three bound vibrational levels have been observed before.[12] We have observed the radiative dissociation of these levels through the repulsive b state. The assignment of the (3,3) band is tentative because the levels are not well known and no ε spectra have been taken on these transition. Table II shows that the $N=1$ and $N=3$ levels, accessed in the $h\leftarrow c$ band, lie just above the dissociation limit. This implies a rather long lifetime for tunneling through the potential barrier. Radiative dissociation is therefore the dominant decay mechanism; the radiative lifetime for $v=2$ has previously been observed to be 18 ns.[9]

The transitions in the $h\leftarrow c$ (4,4) band predissociate by barrier tunneling. Although the $Q3$ transition is hidden under a much stronger peak [$i\leftarrow c,(2,2)R1$], a positive identification could be made through the observation of a predissociation peak at this wavelength. The lifetimes of the $v=4$ levels could not be observed in either the ε or the $h\nu$ peaks, which means 5 ps $<\tau<3$ ns. From this value an upper limit of the barrier width can be calculated.

TABLE II. List of observed new levels in the $h\,^3\Sigma_g^+$ state of H_2. Levels marked with an asterisk (*) are based upon tentative assignments. Numbers in italic denote levels of orthohydrogen. The energy ε above the dissociation limit H(1s)+H(2l) at 118 377.3 cm^{-1} is given in column 4, expressed in meV (8065.47 cm^{-1} per eV), for radiative levels in parentheses. These energies are derived from the c state energies of Table V and the wavelength of the transition (Table I). For the transitions for which a spectrum of released kinetic energy has been recorded, the observed lifetime is given in column 6. A lower limit of 5 ps follows for all levels from the observed width ($\Gamma < 1$ cm^{-1}) and is therefore omitted here. Photon energies (column 4) in italic denote transitions between ortho levels.

	v	N	E (cm^{-1})	ε (meV)	τ (ns)
$h\,^3\Sigma_g^+$	3	*1	*118 397*	(2.4)	
		*3	*657*	(34.7)	
	4	1	*120 307*	239.3	<3
		3	*551*	269.5	<3

E. The $i\,^3\Pi_g$ ($3d\pi$) state

In the case of a Π state, *P*, *Q*, and *R* branches are allowed in transitions from the $c\,^3\Pi_u^-$ state. We observed transitions (see Fig. 3) in the (0,0)-(4,4) bands, up to $N=5$ lower levels. The *i* state is predicted to have a potential barrier with a height of 361 meV for $J=0$.[17] Four vibrational levels lie below the dissociation limit and have accurately been measured by Dieke.[12,14] We have observed their radiative dissociation to the $b\,^3\Sigma_u^+$ state via the continuous ε spectra. The $v=4$ levels are, however, observed to predissociate by barrier tunneling. The new energy levels for $v=4$ are listed in Table III. The lifetimes are determined to lie in the range 5 ps $< \tau <$ 5 ns. The upper limit was 5 ns (and not lower) because the ε resolution in this set of experiments was unfortunately not as good as in most measurements.

In contrast to the other states studied here, an accurate *ab initio* calculation of Kolos and Rychlewski[17] is available for the *i* state potential. We have calculated the energy levels from this theoretical potential curve with a standard Numerov method for $v=4$ and found agreement with our observations within 100 cm^{-1}. This is comparable with the known accuracy of the potential curve for the lower vibrations.[17] The tunneling lifetime for $v=4, N=1$ was calculated to be 3.8 ns and shorter for the higher levels, consistent with our observations. The *i* state also supports a sixth vibration, for which experimental evidence was found recently by Bjerre and Helm[18] and by de Bruijn *et al.*[2]

F. The $j\,^3\Delta_g$ ($3d\delta$) state

The *j* state converges to the H(1s)+H(3l) limit (Fig. 1) like the *g* state. For the *j* state discrete transitions are observed to the first five vibrational levels [(0,0)—(4,4) bands] as indicated in Fig. 3. The *R* 1 branches are most prominent, mainly because this is the only possible transition from the strongly populated $N=1$ level. Only the lowest four vibrational levels, lying below the H(1s)+H(2l) dissociation limit, were previously assigned by Dieke. We observe these levels to dissociate radiatively via the *b* state, a behavior already seen by Eyler and Pipkin[9] for $v=0$. This demonstrates the known strong *l* uncoupling of the 3s-3d complex in H_2 (Ref. 10). A pure Σ←Δ transition is electric dipole forbidden in Hund's case *b*.

We observe the $v=4$ levels to predissociate to H(1s)+H(2l). The ε peak of the *R* 1 transition is shown in Fig. 4 (smooth line), the clearly visible exponential tail (see Sec. III B) could be fitted with $\tau=9$ ns. The measured energy levels and lifetimes are given in Table IV. The lifetimes of the Δ^+ levels [$N=2$ (ortho), $N=3$ (para), etc.] show a gradual decrease from 9 ns ($N=2$) to 5 ns for $N=4$. The $N=3$ (ortho) level is the only Δ^- level for which we have performed an ε measurement. The lifetime is shorter than for the corresponding Δ^+ level. A discussion of the proposed dissociation mechanism, coupling to a (broadened) quasibound level of the $i\,^3\Pi_g$ state, is postponed to Sec. IV.

Fast predissociations and bound-free transitions. At first sight (see Fig. 3), the *j* series seems to end at the (4,4)

TABLE III. List of observed new levels in the $i\,^3\Pi_g$ state of H_2, analogous to Table II. Lifetimes are calculated for barrier tunneling.

	v	N	E (cm^{-1})	ε (meV)	τ (ns) Obs.	τ (ns) Calc.
$i\,^3\Pi_g$	3	*6	*118 779*	(49.8)		
	4	1	119 603	152.0	<5	3.8
		1	*609*	152.7	<5	3.8
		2	*676*	161.0		2.1
		3	797	176.0		0.95
		*3	*852*	182.8		0.95
		4	*957*	195.9	<5	0.35
		5	120 156	220.5	<5	0.11
		6	*392*	249.8	<5	0.03

TABLE IV. List of observed new levels in the $j\,^3\Delta_g$ state of H_2, analogous to Table II. The observed lifetimes given for $v=5$–7 (only for $N=2$) are derived from the width of the optical transition (Table I). The calculated lifetimes are due to rotational coupling with the vibrational continuum of the i state (see text).

	v	N	E (cm^{-1})	ε (meV)	τ (ns) Obs.	Calc.
$j\,^3\Delta_g$	4	2	*120 553*	269.8	9±1	2.8×10^{-2}
		2	555	270.0		2.8×10^{-2}
		3	692	287.0	7.5±1	6.9×10^{-3}
		3	*696*	287.5	4±2	6.9×10^{-3}
		4	*872*	309.3	5±1.5	1.6×10^{-3}
	5	2	*122 280*	484	1×10^{-4}	7.7×10^{-5}
		3	*410*	500		
		3	430	502		
		4	*620*	526		
	6	2	*123 880*	682	1×10^{-4}	9.9×10^{-5}
		2	890	683		
		3	124 010	698		
		4	*430*	750		
	7	2	*125 400*	871	1×10^{-4}	1.1×10^{-4}
		4	*650*	902		
	8	2	*126 770*	1041		
	9	2	*128 090*	1204		

band, all sharp peaks in the wavelength spectrum being assigned to the (0,0)—(4,4) bands of the $j\leftarrow c$ transition. However, as indicated in Fig. 3, a series of "humps" in the photodissociation signal appear that can be assigned as the $R\,1$ transitions of the (5,5)-(9,9) $j\leftarrow c$ bands. These peaks have linewidths of about 50 cm^{-1} (Table I). The energy levels given in Table IV, despite their limited meaning, show that a regular continuation of the j series is found. The predissociation is thus extremely fast, 1×10^{-13} sec. or only about ten vibrational periods. Coupling to the vibrational continuum of the $i\,^3\Pi_g$ state is considered to be responsible for this predissociation as will be discussed further in Sec. IV.

The assignment to high vibrational levels of the j state is supported by the ε measurements. The ε spectra taken on these resonances all exhibit one strong predissociation peak from which the initial rovibrational level of the c state can be calculated using Table V. Spectrum 6*b* is taken at 16 825 cm^{-1}, close to the top of the (5,5) $j\leftarrow c$ $R\,1$ transition. Going to higher photon energies (spectra 6*c*—*e*) gradually the $R\,2$ and later the $R\,3$ transition is seen to dominate as is also indicated in Fig. 3. In spectrum 6*e* even the peaks belonging to $R\,4$ and $R\,5$ appear while $R\,1$ and $R\,2$ have completely vanished. The same behavior is found for the (6,6) R band between 16 650 and 16 800 cm^{-1}. Although it is not evident from the wavelength spectrum all resonances exhibit asymmetric tails. This can be interpreted as Fano profiles[19] (see Sec. IV). While the transition from, for instance, the $v=5, N=1$ level of the c state (which can only be a $R\,1$ transition in the $j\leftarrow c$ band) is observed to disappear from the ε spectra about 100 cm^{-1} above the top of the $R\,1$ resonance [Fig.

TABLE V. Energy levels in cm^{-1} of the metastable $c\,^3\Pi_u^-$ state of H_2, obtained from Dieke (Ref. 12), ($v=0-3$), Kolos and Rychlewski (Ref. 17), and our observed fragmentation energies ε. The values of Dieke are corrected by -149.6 cm^{-1} as given by Miller and Freund (Ref. 14), and from these numbers the corrections ($v=0-3$) for the theoretical levels of Kolos and Rychlewski are found and extrapolated. The rotational level spacings are calculated with the theoretical B_v's and the N dependence is taken equal to the experimental course for $v=3$. The accuracy is estimated to decrease from 1 cm^{-1} for $v=4, N=1$ to a few cm^{-1} for higher values of v and N. The zero level is the $v=0, J=0$ level of the ground state of H_2. Numbers in italic are levels of orthohydrogen (N odd for Π_u^-).

N	$v=4$	$v=5$	$v=6$	$v=7$	$v=8$	$v=9$
1	*103 578*	*105 446*	*107 201*	*108 843*	*110 373*	*111 787*
2	677	540	289	926	451	860
3	*825*	*680*	*422*	*109 051*	*567*	*968*
4	104 020					
5	*260*					

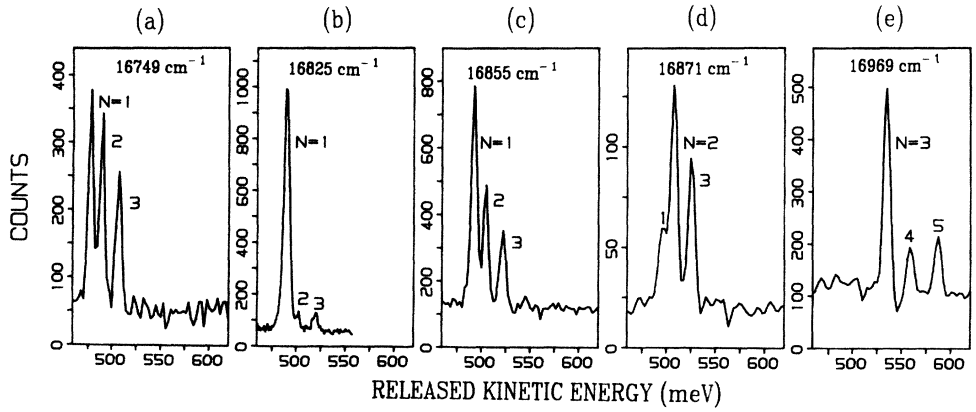

FIG. 6. Predissociation of $v=5$ rotational levels of the $j\,^3\Delta_g$ state of H_2 after excitation of metastable H_2 at various photon energies as indicated at top of the spectra. The rotational quantum numbers (N) in the figure indicate the lower rotational levels involved, belonging to $v=5$ of the $c\,^3\Pi_u^-$ state.

6(e)], it stays present over more than 350 cm^{-1} below the resonance [Figs. 6(a) and 7]. Over the latter range the intensity ratio between the different rotational levels changes as, respectively, the Q- and P-band resonances are passed (not indicated in Fig. 3). In the ε spectrum of Fig. 7, typical for the continuum between 16 300 and 17 000 cm^{-1}, four different vibrational levels of the lower c state are seen to be photodissociated. This spectrum is taken at 16 485 cm^{-1}, not very close to any of the $j \leftarrow c$ resonances except the (6,6) $P3$ transition.

With the evidence discussed above we interpret the continuum in the wavelength spectrum between 16 300 and 17 000 cm^{-1} as being due to simultaneous excitation of the $j \leftarrow c$ (5,5)—(9,9) bands and the i state continuum. Interference between the bound j and continuum i channels leads to the asymmetric Beutler-Fano profiles. In addition to the vibrational continuum of the $i\,^3\Pi_g$ state, the $h\,^3\Sigma_g^+$ and the $a\,^3\Sigma_g^+$ states are accessible in the present wavelength range of which the latter (a $2s$ state lying very close to the c state) can be excluded because the continuum part of the potential is located at too small internuclear distances. The transitions to the h state are weak, as we discussed in Sec. III D. Next to it the pure $h\,^3\Sigma_g \leftarrow c\,^3\Pi_u$ bound-free transition will, in contrast to $i\,^3\Pi_g \leftarrow c\,^3\Pi_u$, exhibit a perpendicular anisotropy[20] which results in a reduced efficiency in the present geometry of the experiment (Sec. II B).

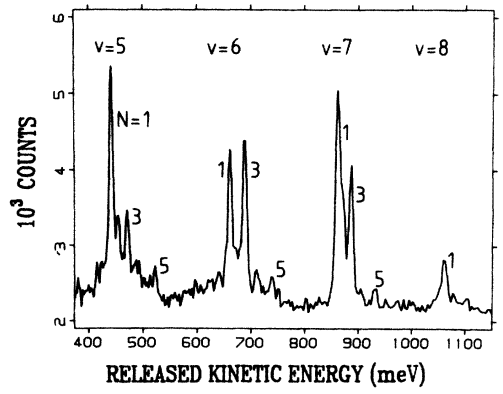

FIG. 7. Spectrum of released kinetic energies after photodissociation of metastable H_2 at 16 485 cm^{-1}. The rovibrational levels of the $c\,^3\Pi_u^-$ lower state are indicated. As discussed in the text, the peaks arise from simultaneous excitation of j state resonances and the i state continuum.

IV. THE PREDISSOCIATION OF THE $v \geq 4$ LEVELS OF THE $j\,^3\Delta_g$ STATE

According to Kronigs selection rules for Hund's case b ($\Delta S=0$, $\Delta\Lambda=0, \pm 1$, $g \not\leftrightarrow u$, and $\Delta N=0$), the pure $j\,^3\Delta_g$ state can only be perturbed by the $i\,^3\Pi_g$ state. For $v \geq 5$ this results in a predissociation because these j levels lie above the potential barrier of the i state. Analogously to Ref. 6 we have calculated the widths of these levels, taking rotational coupling as the perturbing interaction and not including interferences due to simultaneous excitation of the i state continuum,

$$\Gamma(v,N)=2\pi N(N+1)\,|\,\langle\phi_\Pi\,|\,L^+\,|\,\phi_\Delta\rangle\,|^2\xi(v,N)\,, \quad (3)$$

with

$$\xi(v,N)=|\,\langle\chi_\Pi(N)\,|\,-\hbar^2/2\mu R^2\,|\,\chi_\Delta(v,N)\rangle\,|^2\rho(\varepsilon)\,, \quad (4)$$

in which $\rho(\varepsilon)$, the density of states in the continuum, is given by (Ref. 6 gives an expression which is a factor of 2 too small),

$$\rho(\varepsilon)=(2/h)(2\mu/\varepsilon)^{1/2}\,. \quad (5)$$

For the $i\,^3\Pi_g$ state we have used the potential curve of Kolos and Rychlewski.[17] An accurate potential for the $j\,^3\Delta_g$ state is not available. However, the corresponding singlet state ($J\,^1\Delta_g$) has been calculated by Kolos and Rychlewski.[21] By shifting this potential up by only 4 meV the observed triplet levels could be reproduced satisfactorily. The final results for the widths are given in Table I. A strong coupling, in good agreement with the observations for R 1 transitions, are indeed found because there is a strong overlap of vibrational wave functions (see Fig.

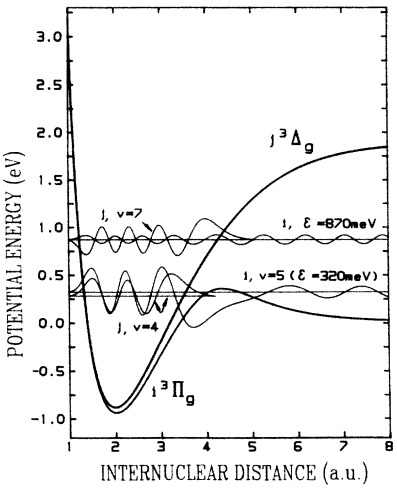

FIG. 8. Illustration of the calculation made on the rotational coupling between discrete j state levels and the vibrational continuum of the i state. Drawn are the vibrational wave functions of $v=4$ and $v=7$ (both $N=2$) of the j state and the free wave functions of the i state ($N=2$) at $\varepsilon=871$ meV and $\varepsilon=320$ meV. The latter energy is at the $v=5$ resonance (quasibound level) of the i state.

8). The strength of this coupling also means that there is actually no pure Δ or Π stated but a mixture to which we excite; as stated before, actually the whole $(3s)\ 3d$ complex is strongly mixed. This results in the series of broad resonances with Fano profiles, caused by the interference of the direct transition to the i state continuum with the path via the predissociative (quasi-) discrete j state level, as observed. The classification of dissociation mechanisms, given in Sec. III B looses its meaning in this special case.

The much slower predissociation of the $v=4$ vibrational levels of the j state is conceptually not different from $v\geq 5$. Rotational coupling to the "vibrational continuum" of the i state is possible but the system is then still separated from dissociation by the potential barrier of the i state (Fig. 8). The lifetime for tunneling at the relevant energies is around 10 ps (following from the i state potential of Ref. 17, including the rotational energy) while the observed lifetimes of the $v=4$ levels of the j state range from 4—9 ns (Table IV). The barrier tunneling is therefore neglected in a calculation of the predissociative lifetimes of the j state levels. The lifetimes for $v=4$ are thus calculated (Table IV) in exactly the same way as for $v\geq 5$. The required i state wave function at the energy of the j state level is calculated, with a standard Numerov method, as a free wave function and normalized at large internuclear distance according to Eq. (5). For clarity the i state wave function in Fig. 8 is given on the resonance for $v=5, N=2$ at $\varepsilon=320$ meV. The wave function which has been used in the calculation, at the energy of the predissociated $v=4, N=2$ j state level of $\varepsilon=270$ meV, has a much smaller amplitude in the potential well. This decrease in amplitude reflects the energy profile of the quasibound $v=5, N=2$ level in the i state, the expected Lorentzian profile with a width of 25 cm^{-1} could be reproduced in this way.

Although the predissociation of the $v=4$ levels is calculated to be more than 2 orders of magnitude slower as for $v\geq 5$, there are still another 2 orders of magnitude lacking in comparing with the experimental values (Table IV). The proposed coupling has to exist but is much *weaker* than calculated here. The i state barrier has to be deformed in a rather dramatic way, far outside the expected accuracy of the theoretical curve, to reduce the coupling (and/or enhance the tunneling time) sufficiently. Most likely the present calculation is too simple for this case. The various couplings to other states[10,22] have to be included in a more rigorous approach. An alternative predissociation mechanism through coupling to the $h\,^3\Sigma_g^+$ state, analogous to the proposed decay of the $J\,^1\Delta_g$ state,[21] would only dissociate the Δ^+ levels (para↮ortho) contrary to our observations.

V. CONCLUSIONS

Fast-beam photofragment spectroscopy has been extended to neutral molecules. The power of this technique, using a two-particle detector, to study dissociative channels in excited states has been demonstrated. The formation of metastable neutral molecules by charge exchange is shown to be very useful. An advantage of this approach is that all vibrational levels can be studied and in this case, excitation from the $c\,^3\Pi_u^-$ state of H_2, electronic states with $S=1$ could be examined which are otherwise almost not accessible. The energies and partly also the lifetimes of 26 levels, which have not been reported before, are measured.

Together with the companion paper,[2] dealing with predissociations of H_2^* following charge exchange of H_2^+ with Cs, an almost complete picture has been generated on dissociations of $n=3$ Rydberg states of H_2. Levels below the $H(1s)+H(2l)$ dissociation limit all decay through photon emission. Only for triplet gerade states this leads to dissociation through the repulsive $b\,^3\Sigma_u^+$ state. Here this decay is observed for the g, h, i, and j states, all existing $n=3$ triplet gerade states. The latter is a $\Sigma\leftarrow\Delta$ transition which is allowed through strong l uncoupling. In principle triplet ungerade and singlet gerade states (e.g., the low-lying e and G,K $n=3$ states) can predissociate to the $H(1s)+H(1s)$ dissociation limit through the b and ground states, respectively. The coupling will, however, not be very strong because the initial and final states do not merge at small internuclear distances. Besides the predissociation of the $c\,^3\Pi_u^+$ $(2p\pi)$ state no evidence has been found for this process.[5]

For levels of $n=3$ states above the $H(1s)+H(2l)$ dissociation limit predissociation to this limit is an important decay channel. Mainly for Λ^- parts of Π and Δ states fluorescence is the decay mechanism because they cannot be predissociated by Σ^+ states. Only for $v\geq 7$ of the d state autoionization is observed.[2] Predissociation is described in the companion paper for the $d\,^3\Pi_u^+$, the $D\,^1\Pi_u^+$, and the $J\,^1\Delta_g^+$ and in the present communication

of the $j\,^3\Delta_g$ state. In both experiments predissociation of the quasibound levels of the $h\,^3\Sigma_g^+$ ($v=4$) and $i\,^3\Pi_g$ ($v=4,5$) states are observed. The only $n=3$ state, converging to the H(1s)+H(3l) limit, which is not yet mentioned here is the $g\,^3\Sigma_g^+$ state. Levels of this state above the dissociation limit could not be observed in the present wavelength range. These levels could be predissociated by the $i\,^3\Pi_g$ state, fluorescence is not reported by Dieke.[11]

The $v \geq 5$ levels of the j state are very rapidly ($\tau \simeq 10^{-13}$ s) predissociated by the i state. Calculations of the rotational coupling between these states showed a good agreement with the observed lifetimes. The relatively slow ($\tau \leq 9$ ns) predissociation of the fourth vibrational level, observed for both the Δ^+ and the Δ^- components, is not fully explained. The calculation of the rotational coupling to the i state, at energies below its barrier, delivered a much weaker coupling than for $v \geq 5$ but still much too large compared with the experiment.

In these experiments the anisotropy of the photodissociation has not been measured. As explained in Sec. III B, the polarization of the laser was chosen perpendicular to the ion beam for practical reasons, while a parallel orientation is required for meaningful angular spectra. We plan to perform such measurements in the near future. It will be particularly interesting to study the variation of the anisotropy across the Beutler-Fano profiles of the j state resonances.

ACKNOWLEDGMENTS

We acknowledge technical support by H. Pape and L. de Boer and the continuous encouragement of J. Los. We also thank T. R. Govers for the discussions which have led to this experiment and W. Koot for helpful discussions to explain the results. This work is part of the research program of the Foundation for Fundamental Research on Matter (FOM) and was made possible by financial support of the Dutch Organization for the Advancement of Pure Research (ZWO) and also the National Science Foundation through Grant No. PHY84-11517.

---

*Present address: Koninklijkelshell-Laboratorium, Postbus 3003, 1003 AA Amsterdam, the Netherlands.

†Permanent address: Molecular Physics Department, SRI International, Menlo Park, CA 94025.

[1]H. Helm, D. P. de Bruijn, and J. Los, Phys. Rev. Lett. **53**, 1642 (1984).

[2]D. P. de Bruijn, J. Neuteboom, T. R. Govers, and J. Los, preceding paper, Phys. Rev. A **34**, 3847 (1986).

[3]D. P. de Bruijn and J. Los, Rev. Sci. Instrum. **53**, 1020 (1982).

[4]D. P. de Bruijn, J. Neuteboom, V. Sidis, and J. Los, Chem. Phys. **85**, 215 (1984).

[5]D. P. de Bruijn, J. Neuteboom, and J. Los, Chem. Phys. **85**, 233 (1984).

[6]G. Comtet and D. P. de Bruijn, Chem. Phys. **94**, 365 (1985).

[7]C. E. Johnson, Phys. Rev. A **5**, 1026 (1972).

[8]R. P. Freis and J. R. Hiskes, Phys. Rev. A **2**, 573 (1970).

[9]E. E. Eyler and F. M. Pipkin, Phys. Rev. Lett. **47**, 1270 (1981).

[10]M. L. Ginter, J. Chem. Phys. **46**, 3687 (1967).

[11]G. H. Dieke, J. Mol. Spectrosc. **2**, 494 (1958).

[12]H. M. Crosswhite, *The Hydrogen Molecule Wavelength Tables of Gerhard Heinrich Dieke* (Wiley, New York, 1972).

[13]G. Herzberg, Sci. Light (Tokyo) **16**, 14 (1967).

[14]T. A. Miller and R. S. Freund, J. Chem. Phys. **61**, 2160 (1974).

[15]E. U. Condon and G. H. Shortley, *The Theory of Atomic Spectra* (Cambridge University Press, London, 1959).

[16]T. E. Sharp, At. Data **2**, 119 (1971).

[17]W. Kolos and J. Rychlewski, J. Mol. Spectrosc. **66**, 428 (1977).

[18]N. Bjerre and H. Helm, *Book of Abstracts of the Second European Conference on Atomic and Molecular Physics,* edited by A. E. de Vries and M. J. van der Wiel (Free University Press, Amsterdam, 1985), p. 169.

[19]U. Fano, Phys. Rev. **124**, 1866 (1961).

[20]S. Mukamel and J. Jortner, Chem. Phys. Lett. **29**, 169 (1974).

[21]W. Kolos and J. Rychlewski, J. Mol. Spectrosc. **91**, 128 (1982).

[22]R. S. Mulliken, J. Am. Chem. Soc. **88**, 1849 (1966).